Interdisciplinary Sciences: Computational Life Sciences (2022) 14:804–813
https://doi.org/10.1007/s12539-022-00531-1

ORIGINAL RESEARCH ARTICLE

Diagnosis of Pancreatic Cancer Using miRNA30e Biosensor

Namita Sharma[1] · **Sudha Srivastava**[1]

Received: 2 December 2021 / Revised: 27 May 2022 / Accepted: 1 June 2022 / Published online: 3 July 2022

Abstract

This work describes miRNA-based electrochemical biosensor for detection of miRNA30e, a pancreatic cancer biomarker. The screen-printed gold electrode was functionalized using cysteine hydrochloride followed by immobilization of synthesized colloidal gold nanorods (10–12 nm diameter and 25–65 nm length). The gold nanorods modified electrode surface was amino functionalized for covalent attachment of single-stranded DNA probe against miRNA30e (miR30e). This platform was utilized for electrochemical measurements and response analysis of target miRNA30e. Electrochemical impedance spectroscopic measurements showed very poor sensitivity (13.51 Ω/µg/mL/cm^2) using charge transfer resistance calibration plots. Cyclic voltammetry and differential pulse voltammetry-based miR30e quantification showed decreasing current response with increasing concentration of miR30e with detection range of 0.1 fg/mL–0.1 µg/mL (14.9 aM–14.9 nM). The sensitivity of DPV sensing (104.4 µA/µg/mL/cm^2) was found to be 1.3 times higher than that of CV-based quantification (79.6 µA/µg/mL/cm^2). miRNA-based biosensors have the potential of replacing current invasive, time consuming and technically difficult diagnostic procedures. Furthermore, the lower limit of detection of 14.9 aM miRNA30e makes it a promising tool for detection of cancer at early stages and hence increasing survival rate.

Graphical Abstract

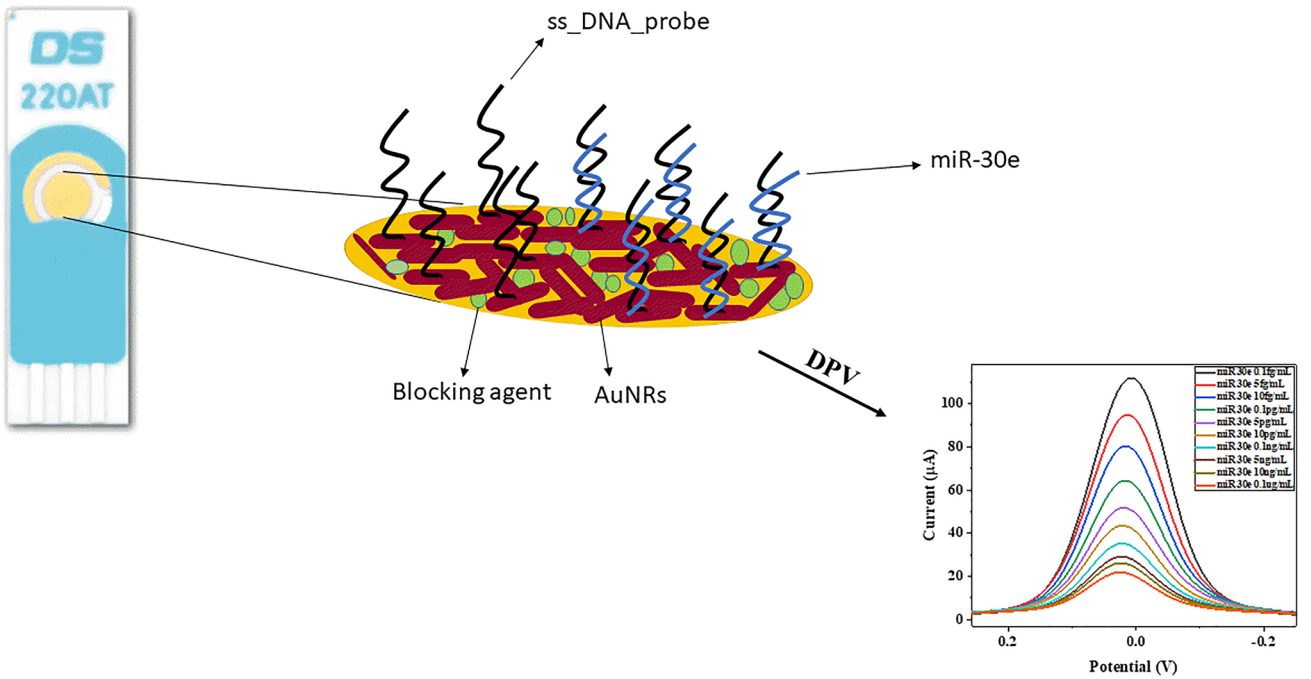

Keywords miR30e · Electrochemical impedance spectroscopy · Biosensor

Extended author information available on the last page of the article

1 Introduction

With technological advancements in diagnostic methods, survival rates of most of the cancers have improved. However, pancreatic cancer is still considered deadliest (7% of cancer death), despite its low occurrence (3% of diagnosed cancer cases). In India, prevalence of pancreatic cancer is as low as 0.5–2.4 in 100,000 persons/year; however, 5-year survival rates of < 5% make it a point of concern [1]. This could be attributed to the difficulty in early diagnosis because of its positioning, i.e., between stomach and spine, surrounded by small intestine, liver, bile duct, spleen gallbladder, making it difficult to identify any tumor/growth through physical examination. Pancreatic cancer is majorly of two types—endocrine tumors and exocrine tumors. Endocrine tumors (also known as pancreatic neuroendocrine tumors (PNETs) or islet cell tumors) comprise of only 7% of pancreatic cancer, while remaining ~ 93% is exocrine pancreatic cancer (majorly—pancreatic ductal adenoma carcinoma or adenocarcinoma (PDAC); other rare ones—colloid carcinoma, adenosquamous carcinoma and squamous cell carcinoma).

Various imaging techniques are used as the first diagnostic and screening tool. Abdominal ultrasound being non-invasive, inexpensive and no side effects of any contrast agents, is most common procedure for pancreatic cancer diagnosis; however, its accuracy is only 50–70% [2]. Computer tomography (CT) is another widely used technique for suspected cases of pancreatic cancers. Non-contrast CT has poor sensitivity and specificity but phase contrast CT has high sensitivity of 76–92% [3]. Another equally sensitive technique for pancreatic cancer diagnosis is magnetic resonance imaging (MRI) having sensitivity of 84% which is done in addition/prior to tissue biopsy. Positron emission tomography (PET) imaging is done along with CT, and improved sensitivity of 87–95% and specificity of 51–81% are achieved [4]. However, all these imaging methods require trained manpower and expensive instruments while tissue biopsy has an additional drawback of being invasive in nature.

Pancreatic cancer can be diagnosed using protein biomarkers present in blood or urine such as CA 19-9 [5], CEA [6], and HE4 [7]. Among these, CA19-9 is the only biomarker that has been approved by US FDA for prognosis of pancreatic cancer, though its specificity is low. In addition, CA19-9 can be absent or low in Lewis's antigen-negative patients [8] in addition to protein biomarkers, cell-free DNA (cfDNA) and miRNA have also been identified for diagnosis and/or prognosis of pancreatic cancer. Genetic mutations in ERBB2 Exon 17, ERBB2 exon27, BRCA2, EGFR, KDR, KRAS G12, KRAS G12V, KRAS G12D, and KRAS G12R have been reported in pancreatic cancer. Mutation in KRAS genes in PDAC were diagnosed in 1990s itself but till date, its significance as diagnostic biomarker, in unresectable PDAC cases, is not established [9] though can be used as prognostic biomarker. Furthermore, methylation in cfDNA is also being employed as diagnostic marker since it occurs at very early stage; however, its adaptation in diagnostic devices is restricted due to sample sequencing requirement and other associated technical limitations. In addition, heterogeneity in the cfDNA or circulating tumor DNA renders it difficult to analyze the data without combining it with epigenetic information [10]. miRNA, small stretches of noncoding RNAs, have emerged as promising biomarkers though specificity of individual miRNAs is still debatable. miRNAs were first discovered in 1990s though its role as distinct class of biological regulators was established in 2000s [11–14]. Dysregulated expression of miRNA expression is strongly correlated with various diseases including cancer [15]. Some of the miRNA-based biomarkers identified in blood samples of pancreatic cancer patients are miR196a [16], miR196b [16], miR1246 [17], miR25 [18], miR194 [19], miR192 [20], miR21, miR155, miR221, miR100, and miR181b [21], miR 221-3p [22], miR18a [23], miR1290 [24], miR22-3p, miR642b-3p, miR885-5p [25], miR200a and miR200b [26], miR215-5p, miR122-5p, miR192-5p, miR30b-5p, miR320b [27], miR181a, miR181b, miR106b [28], miR483-3p [29], miR486-5p, miR126-3p, miR26b-3p, miR181c-5p, and miR938 [30]. Debarnardi and coworkers [31] reported miR30e, miR143, miR223 and miR204 as miRNA biomarkers for pancreatic adenocarcinoma.

Electrochemical biosensors have emerged as a powerful tool for quick and easy detection of biomarkers. miRNA-based biosensor was first reported in 2006, since then researchers have employed electrochemical quantification of miRNA biomarkers for breast, gastric, pancreatic, lung, colorectal, prostrate, hepatocellular carcinoma, and cervical cancer [32]. miR21 biomarker present in PDAC as well as in other cancers, was detected upto 1 fM concentration using gold nanoparticles and carbon black-modified pencil graphite electrode [33]. Another PDAC miRNA biomarker—miR196b was electrochemically quantified using a hairpin probe on polydopamine–gold composite with detection limit 0.26 pM [34]. Detection limits of miRNA detection were further improved to 15 aM levels by combining cyclic enzymatic amplification and template-free DNA extension reaction with electrochemical sensing [35]. The sensitivity of miRNA-based detection for discrimination between PDAC and healthy individuals was improved using panel of miR rather than single miR biomarker. Zeng and coworkers [36] employed probe DNA tetrahedral nanostructures to develop biosensor panel of miRNAs for pancreatic cancer—miRNA 155,

miRNA 21, miRNA 196A and miRNA 210 simultaneously the detection limit of 10 fem.

Here, we report an electrochemical biosensor for detection and quantification of miR30e spiked in FBS sample to mimic clinical samples. miR30e is a member of microRNA-30 (miR30) family, comprising of six mature miRNA molecules—miR30a, miR30b, miR30c-1, miR30c-2, miR30d, and miR30e. It was found that this family plays a vital role in tissues and organs development, cell differentiation, cellular senescence, apoptosis, cancer, cardiovascular diseases, renal disease, respiratory disorders, and other clinical diseases [37, 38]. miR30e was found significantly in higher amounts in the urine of pancreatic cancer Stage I patients compared to the healthy population [31]. Its level was significantly upregulated in the plasma exosome of patients with atherosclerosis [39]. Lower expression of miR30e was found during breast cancer, nasopharyngeal carcinoma, which enhances migration, proliferation, and invasion of tumor cells [38, 40]. Significantly lower expression level of miR30e was also found in hepatocellular carcinoma as compared to severe liver disease and healthy individuals [41]. In diabetic kidney disease (DKD), the expression level of miR30e was found downregulated in urine and plasma samples of patients [42]. Hence, elevated levels of miR30e in urine samples can be correlated with pancreatic cancer progression. In the present work, single-stranded probe DNA complimentary to miR30e was immobilized on gold nanorods modified screen-printed gold electrodes followed by electrochemical response analysis using EIS, CV and DPV for quantification of miR30e. Fabricated immunosensor could detect miR30e to as low as 0.1 fg/mL concentration.

2 Experimental

2.1 Instrumentation and Reagents

All electrochemical measurements were performed on CHI604E electrochemical workstation (CH Instruments Inc., USA) controlled by its software. The screen-printed gold electrode (DRP220AT) was purchased from DropSens. The working and counter electrodes were made of gold, and reference electrode of silver (Ag/AgCl) with electrical contacts of silver. UV/Vis spectrophotometer (Jenway) was used for optical characterization of gold nanoparticles.

Tetrachloroauric acid ($HAuCl_4.3H_2O$), trisodium citrate dihydrate, cysteine hydrochloride ($CH_2(SH).CH(COOH).NH_2.HCl$) and probe DNA and miRNA were purchased from Sigma-Aldrich. These buffer solutions were prepared in MilliQ water (18 MΩ cm at 25 °C). Tris-(hydroxymethyl) aminomethane (Tris), ethylenediaminetetraacetic acid (EDTA), potassium ferrocyanide ($K_4Fe(CN)_6$), potassium ferricyanide ($K_3Fe(CN)_6$) were purchased from Himedia Laboratories Pvt. Ltd. Sodium chloride (NaCl), Potassium chloride (KCl), Disodium hydrogen phosphate (Na_2HPO_4), Potassium dihydrogen phosphate (KH_2PO_4), gelatin, and Tween 20 were procured from CDH Chemicals. Stock solutions of oligonucleotides (100 µM) were prepared in Tris−EDTA buffer and were stored at − 20 °C. All solutions were stored at 4 °C when in regular use.

2.2 Gold Nanorods' Synthesis

Gold nanorods' synthesis was carried out by reduction of gold precursor with butyric acid. 2 mL of 5 mM aqueous solution of gold precursor (tetrachloroauric acid solution) was added in a conical flask containing 100 mL of boiling MilliQ water. Solution was vigorously mixed to ensure uniformly mixed solution. Au (III) was reduced to Au (0) state by 0.1 mL/min addition of 100 mM butyric acid (3 mL) at while solution was vigorously mixed on the magnetic stirrer. On addition of butyric acid, color of the solution changes from pale yellow to violet. With addition of more and more reducing agent, the color changes greyish black and eventually dirty orange-colored colloidal suspension. This suspension was quenched by immersing the flask in an ice bucket and sonicated for 15 min in ultrasonic water bath. The suspension was centrifuged at 9000 rpm for 15 min and the pellet was resuspended in 100 µL of milliQ water.

2.3 Fabrication of NH_2-ssDNA/AuNRs/SPGE

The screen-printed gold electrode from DropSens (DRP220 AT) was used to fabricate DNA-based biosensor. The three-electrode system consisted of working and counter electrode made of gold, while reference electrode was of silver with electrical contacts made of silver. The electrode working surface was cleaned using ethanol, then rinsed with MilliQ water. This was followed by addition of 10 µL of cysteine hydrochloride (2 mg/mL) which was added to the surface and incubated for 1 h in dark. Addition of gold nanorods (AuNRs) onto the cysteine hydrochloride-modified electrode surface results in monolayer of AuNRs on working electrode. Physically adsorbed AuNRs were removed by rinsing the electrodes 2–3 times with MilliQ water. This was followed by addition of 10 µL of 0.5 µg amino-terminated ssDNA probe (AmC_6 5′ACATTTGTAGGAACTGAC CTTC3′) and incubated for 1 h. This step forms a covalent linkage between gold nanorods and the single-stranded probe DNA. The electrode surface was blocked by 2% gelatin prepared in 0.1% tween 20 with PBS (0.01 M, pH 7.4) and incubated for 1 h at 37 ºC. Finally, the electrode was washed with water and stored in 0.01 M PBS (pH 7.4) at 4 ºC till further use. Figure 1 shows schematic representation of stepwise fabrication of electrodes.

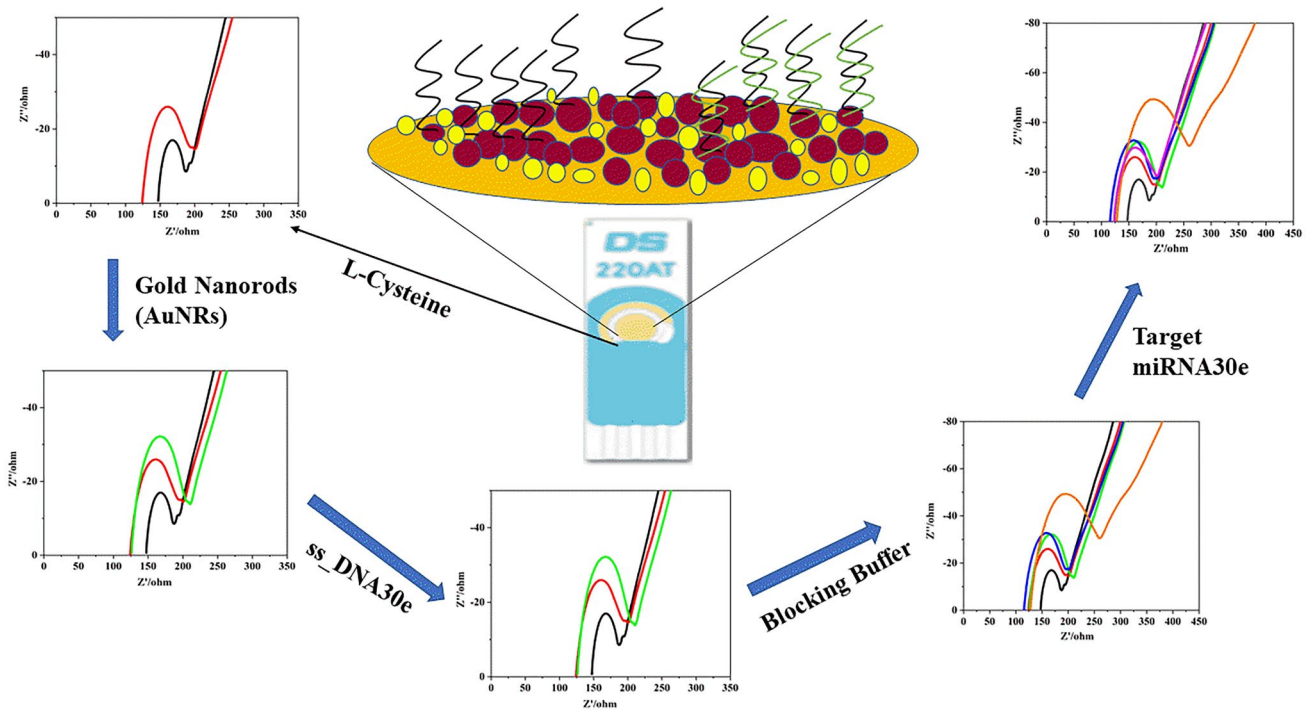

Fig. 1 Schematic representation of gold electrode fabrication for miR30e biosensing

2.4 Impedance Measurements

The electrochemical impedance spectroscopy (EIS) was performed using electrochemical workstation CHI604E from CH Instruments Inc, USA. AC impedance measurements were done by varying frequency from 100,000 Hz to 1 Hz at an applied potential of 15 mV and amplitude 0.005 V. 12 points per decade of frequency were recorded to generate EIS spectra in 5 mM $[Fe(CN)_6]^{3-/4-}$ electrolyte solution.

Time of hybridization of single-stranded probe immobilized on fabricated biosensor and corresponding miRNA30e was optimized by adding 10 µL of 0.5 µg/mL miR30e (5′GAAGGUCAGUUCCUACAAAUGU 3′) prepared in 0.01 M PBS pH 7.4, onto working electrode. This was followed by addition of 100 µL of 5 mM $[Fe(CN)_6]^{3-/4-}$ electrolyte solution covering all three electrodes and recording the EIS spectra. For quantification of miR30e, different concentrations (0.1 fg/mL–0.1 µg/mL) were prepared in FBS solution to mimic the clinical samples and EIS spectra was recorded at 30 °C.

2.5 Voltammetric Measurements

Cyclic voltammetric (CV) measurements were carried out in 5 mM $[Fe(CN)_6]^{3-/4-}$ electrolyte solution, scanning the potential from 0.8 to − 0.8 V at a rate of 0.1 V/s. The differential pulse voltammetric (DPV) measurements were done over a potential window of 0.3 to − 0.3 V with increment of 0.004 V, amplitude 0.05 V and pulse width of 0.05 V. Finally, CV and DPV measurements were carried out for different samples of miR30e (0.1 fg/mL–0.1 µg/mL) prepared by spiking it in FBS and recording the spectra.

3 Results and Discussion

3.1 Design and Characterization of miRNA-Based Biosensor

The electrochemical detection of miR30e is reported first time in this paper. The gold screen-printed electrode (SPGE) is used to design the electrochemical biosensor. The thiol group of L-cysteine hydrochloride (CH_2(SH).CH(COOH).NH_2.HCl) forms Au–SH bond with the bare gold electrode surface. The freely available amine group of cysteine hydrochloride, forms amide linkage with citrate capped gold nanorods (AuNRs). Figure 2a shows TEM micrograph of rod-like nanostructures with an aspect ratio of ~ 2.5 having diameter of 12–20 nm and length 25–65 nm with inset showing size distribution of AuNRs, while UV–visible absorption spectra showing a broad band with maxima around 520 nm and a small hump at 540 nm indicative of rod-like structure is shown in Fig. 2b. These self-assembled monolayers of gold nanorods are further covalently linked to amino tagged ssDNA probe (ssDNA 30e) through amide bond formation. To avoid non-specific interaction, electrode surface was

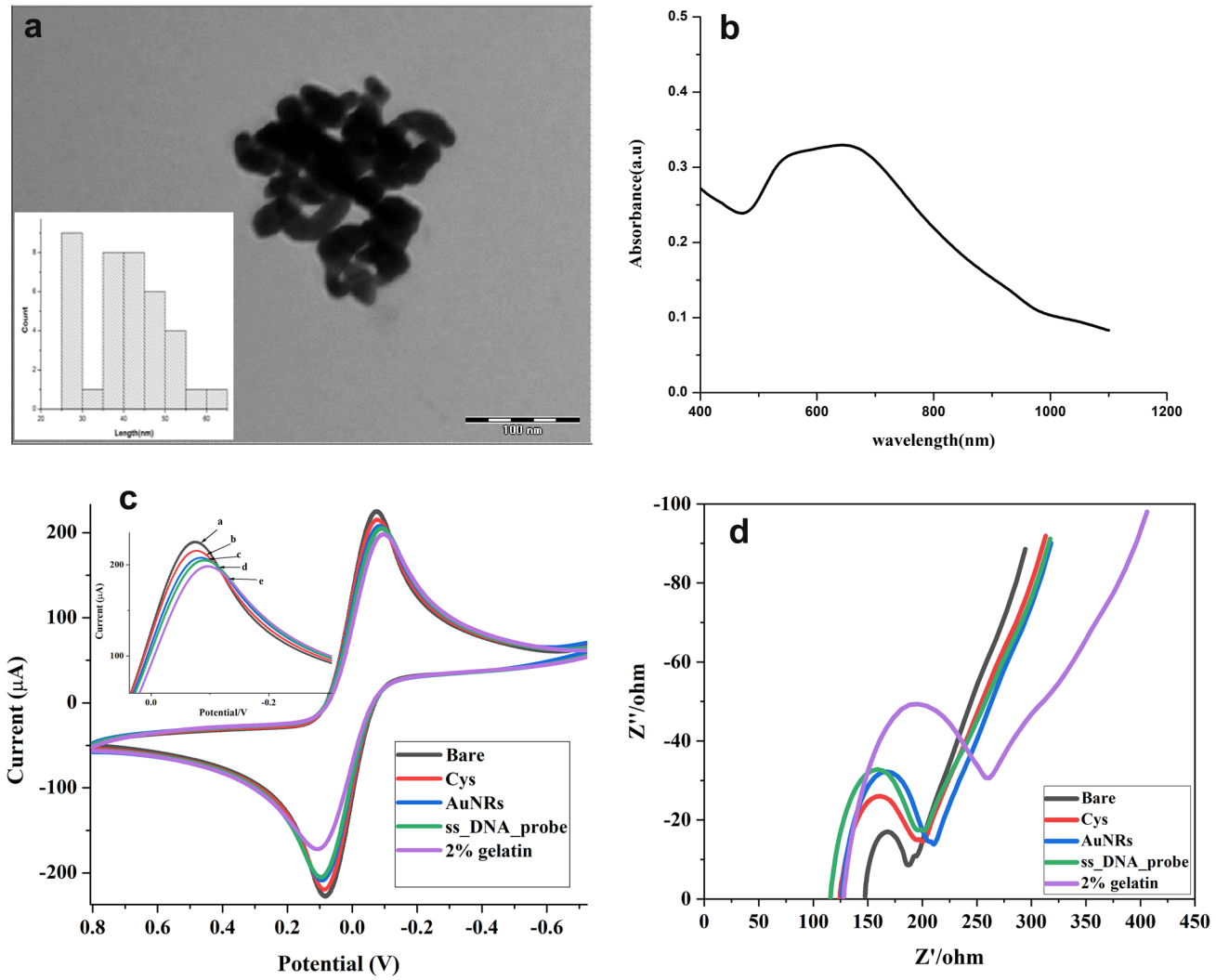

Fig. 2 **a** Transmission electron microscopic image of gold nanorods. Inset shows size distribution(length) of the AuNRs, **b** UV–visible absorption spectra of the synthesized gold nanorods, **c** CV and **d** EIS measurements after each fabrication step of SPGE (SPGE, CysHCl/SPGE, AuNRs/CysHCl/SPGE, ssDNAprobe/AuNRs/CysHCl/SPGE, and after blocking). Signals were recorded in the presence of ferri-ferrocyanide

blocked using gelatin as a blocking agent. Finally, presence of miR30e in spiked in FBS sample was evaluated by electrochemical analysis of hybridization of miR30e with its probe on electrode surface.

The chemical modification at each step was confirmed by electrochemical characterization techniques—using cyclic voltammetry (CV, Fig. 2c) and electrochemical impedance spectroscopy (EIS, Fig. 2d). As shown in Fig. 2c, bare screen-printed gold electrode (black-colored line) showed the redox peaks of ferri/ferrocyanide electrolyte at − 0.074 V (cathodic, E_{pc}) and 0.082 V (anodic, E_{pa}). Modification of electrode surface with linker molecule cysteine results in formation of a strong Au–S bond between cysteine sulfur atom and the gold electrode surface. The self-assembled monolayer of cysteine on the gold electrode was marked by decrease in peak current to 215 μA (red-colored curve) as compared to 225 μA for bare electrode. In addition to this, a marginal shift in peak potential was also observed (*E*pc: − 0.0773 V and E_{pa}: 0.085 V) leading to decrease in peak potential difference (ΔE_p). The current.

response further decreases after the immobilization of AuNRs (blue-colored curve) to 207 μA with increased peak separation (E_{pc}: − 0.085, E_{pa}: 0.094) indicative of sluggish reaction rates. Finally, immobilization of ssDNA probe was confirmed by further reduction in current response to 205 μA (green-colored curve) and the redox peak potential separation also increased further (E_{pc}: − 0.091, E_{pa}: 0.095). Blocking of electrode with blocking agent (2% gelatin in Tween 20 buffer) increases the insulating like character at the electrode surface thereby reducing the current response

further as marked by reduction in peak current to 181 µA (purple-colored curve).

Electrode fabrication was further confirmed by electrochemical impedance spectroscopic analysis. Figure 2d shows EIS response, depicting resistive process in terms of Nyquist plot, i.e., variation of real impedance (Z') and imaginary impedance ($-Z''$) at different excitation frequency ω [43]. Solution resistance (Rs) was found to be 116 Ω and the charge transfer resistance (R_{CT}) at the bare electrode was obtained as 42 Ω (black-colored curve). As observed from Fig. 2d, modification of the electrode surface with L-cysteine results in increase in charge transfer resistance (R_{CT}) at the interface to 71 Ω (red-colored curve). This agrees well with the observation of decreased peak current response of cysteine-modified electrode surface (as observed in Fig. 2c, red-colored curve). Immobilization of gold nanorods onto electrode surface resulted in further increase in R_{CT} (82 Ω). Finally, single-stranded probe DNA immobilization was marked by further increase in R_{CT} to 98 Ω that increased further to 125 Ω after blocking of the electrode surface using 2% gelatin.

3.2 Analytical Performance of miRNA30e Biosensor

Analytical performance of the fabricated biosensor was evaluated using impedance spectroscopy, cyclic voltammetry and differential pulse voltammetry. Detection and quantification of miRNA30e was performed by adding increasing concentrations of miRNA sample spiked in fetal bovine serum (to mimic real life sample matrix) over the working electrode surface.

Impedimetric response of the miRNA biosensor was recorded for different concentrations of miR30e from 0.1 fg/mL to 0.1 µg/mL and the Nyquist plot for the same is shown in Fig. 3a. As observed from Fig. 3a resistance to charge transfer offered by the electrode surface increases with increasing concentration of miR30e. This can be understood in terms of the decreased charge transfer through purine–pyrimidine base-stacking in case of dsDNA in comparison to the charge transfer through single-stranded DNA nucleobase-stacking [44]. The charge transfer resistance was plotted as a function of miR30e concentration as shown in calibration plot Fig. 3b. EIS-based biosensor exhibits a dynamic detection range from 0.1 fg/mL to 0.1 µg/mL (14.9 aM–14.9 nM) with two-step linearity over the entire dynamic range (as shown in Fig. 3b, red solid lines). Observed limit of detection of 15 aM is better than other reported EIS-based miR25 biosensor having LOD of 0.25 pM [45], However, sensitivity of present biosensor is poor with charge transfer resistance showing a marginal increase from 23.9 to 40 Ω for change in miR30e concentration from 0.1 fg/mL to 0.1 µg/mL. This minimal change in charge transfer resistance upon hybridization with miR30e can be explained in light of the study by Zhuravel and Co-workers [46] on charge transfer analysis of double-stranded DNA and nicked DNA. It was reported that charge transfer was regulated by single DNA backbone only and hybridization has minimal effect on charge transfer. Hence, calibration plot using charge transfer resistance for miR30e quantification is not a good choice. To improve the sensitivity of miR30e biomarker quantification, voltammetric techniques were evaluated.

Fabricated biosensor performance was evaluated by recording cyclic voltammetric response of miR30e spiked

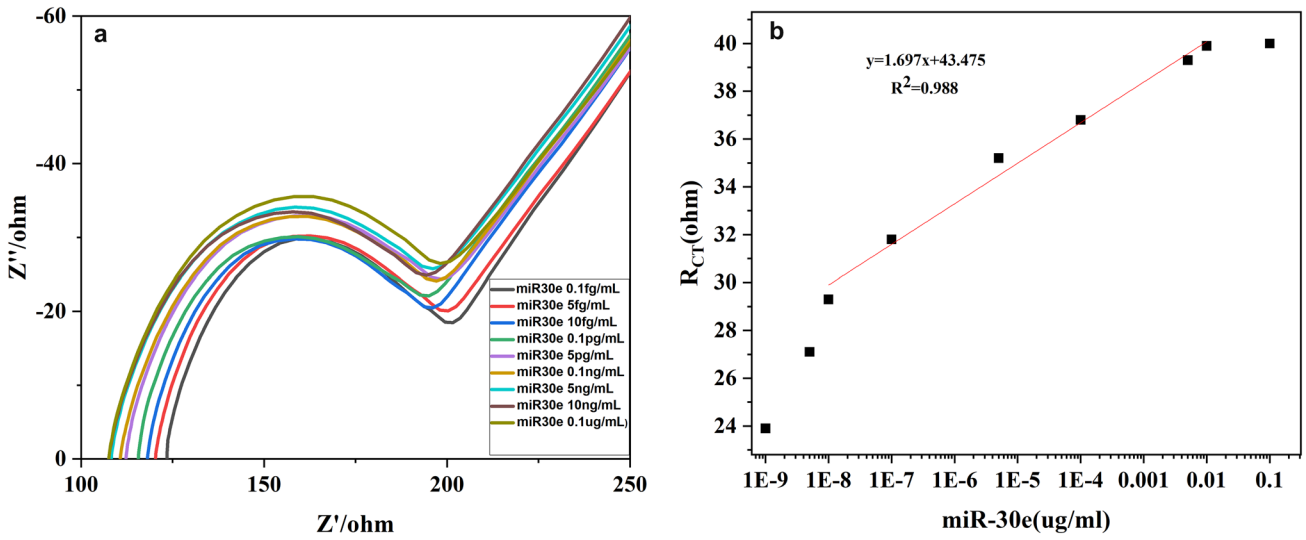

Fig. 3 **a** Nyquist plot of real vs imaginary impedance with increasing concentration of miRNA30e (0.1 fg/mL to 0.1 µg/mL) spiked in FBS. **b** Calibration plot showing charge transfer resistance as a function of target miRNA30e concentration

in FBS over a concentration range of 0.1 fg/mL–0.1 µg/mL. Figure 4a shows redox peaks at − 0.121 V and 0.117 V with ΔE_p of 0.238 V. As the concentration of miR30e in the FBS sample increased, the cathodic peak potential showed a marginal shift towards higher potential (from − 0.121 V to − 0.172 V) while no change in anodic peak potential was observed. This is indicative of diffusion dependent quasi-reversible process. That was further substantiated by the fact that cathodic and anodic peak current were not same and ratio of $I_{pc}/I_{pa} = 161\ \mu A/150\ \mu A = 1.07 \neq 1$. The calibration plot of peak current as a function miR30e concentration is shown in Fig. 4b. With increasing concentration of miR30e in the FBS sample, hybridization with probe DNA on the electrode surface increases resulting in increased density of anionic phosphate backbone. The increased presence of negative ions on electrode surface enhances the barrier potential for electron transfer. The dynamic range observed to be same as that in EIS-based detection; however, an improvement in linear range (LR) was observed in cyclic voltammetric measurements, i.e., 5 fg/mL to 0.1 µg/mL (75 aM–14.9 nM). Sensitivity of the fabricated biosensor was observed to be 79.6 µA/µg/mL/cm^2. Observed linear as well as dynamic range of cyclic voltammetry response was much better than other reported pancreatic biomarkers—CV-based miR133b biosensor (LR: 10 fM–520 pM; LOD: 29 fM) [47], amperometry-based miR21 biosensor (LR: 96 fM−25 pM) [48] and square wave voltammetry-based miR196b biosensor (LR: 1 pM–10 nM; LOD: 0.26 pM) [34].

miRNA concentration is quite low in blood samples; hence, differential pulse voltammetry was employed to explore if any further improvement in detection limits could be achieved. Differential pulse voltammetric measurements were done over the potential window of − 0.3 to 0.3 V, scanning the cathodic peak. Figure 5a shows variation DPV response curves with varying concentration of miR30e. As observed, peak current decreases with increasing biomarker concentration. The calibration plot for the DPV current response is shown in Fig. 5b. Sensitivity of the biosensor improved to 104.4 µA/µg/mL/cm^2 in comparison to 79.6 µA/µg/mL/cm^2 observed in cyclic voltammetric response analysis. DPV-based quantification.

3.3 Interference Analysis

The selectivity of miRNA30e biosensor was evaluated using complementary targets (miR30e), non-complementary targets (miR143, miR204) and *E. coli* genomic DNA as negative control on modified screen-printed gold electrode. Figure 6 shows current response of biosensor after spiking 0.1 µg/mL of miR30e in FBS and same amount of non-specific or interfering molecules—miR143, miR204 and *E. coli* genomic DNA. Percentage interference of miR143, miR204 and *E. coli* genomic DNA was observed to be 2.35%, 1.35% and 3.59%, respectively, considering response of same quantity of target miR30e spiked FBS sample as 100%.

4 Conclusion

In this work, we have proposed gold nanorods modified miRNA30e-based biosensor for diagnosis of pancreatic cancer. The charge transfer resistance shows monotonously increasing behavior with increasing miR30e biomarker concentration in the FBS sample. Fabricated biosensor displays wide dynamic range from 14.9 aM to 14.9 nM and sensitivity of 104 µA/µg/mL/cm^2, respectively. CV- and

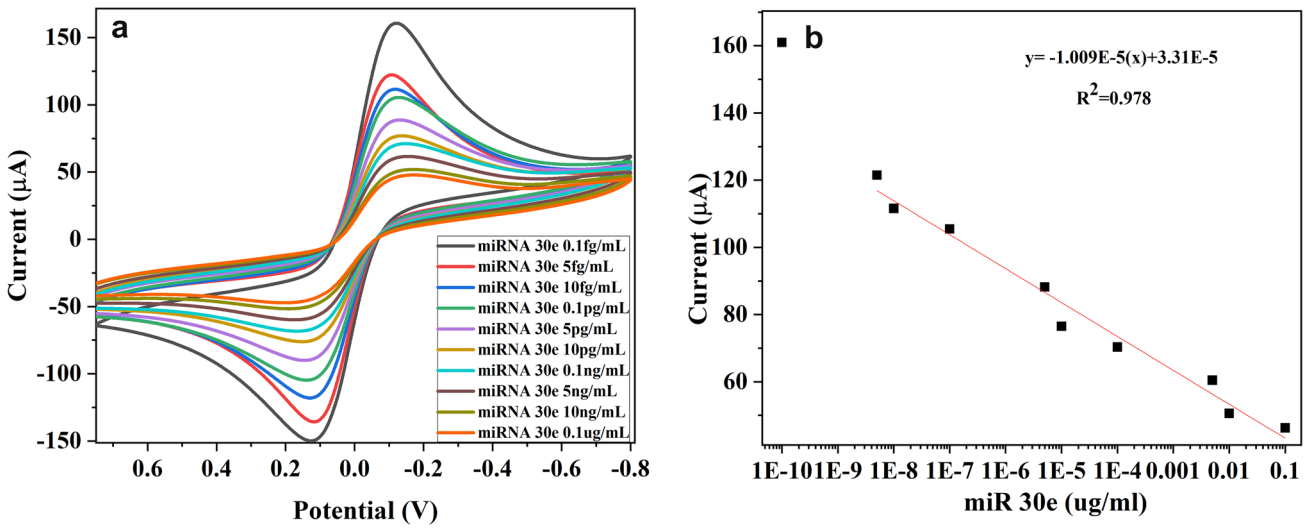

Fig. 4 **a** Cyclic voltammogram showing current response of fabricated biosensor after spiking FBS with different concentrations of target miRNA30e (0.1 fg/mL to 0.1 µg/mL). **b** Calibration plot of peak current as a function of miR30e concentration

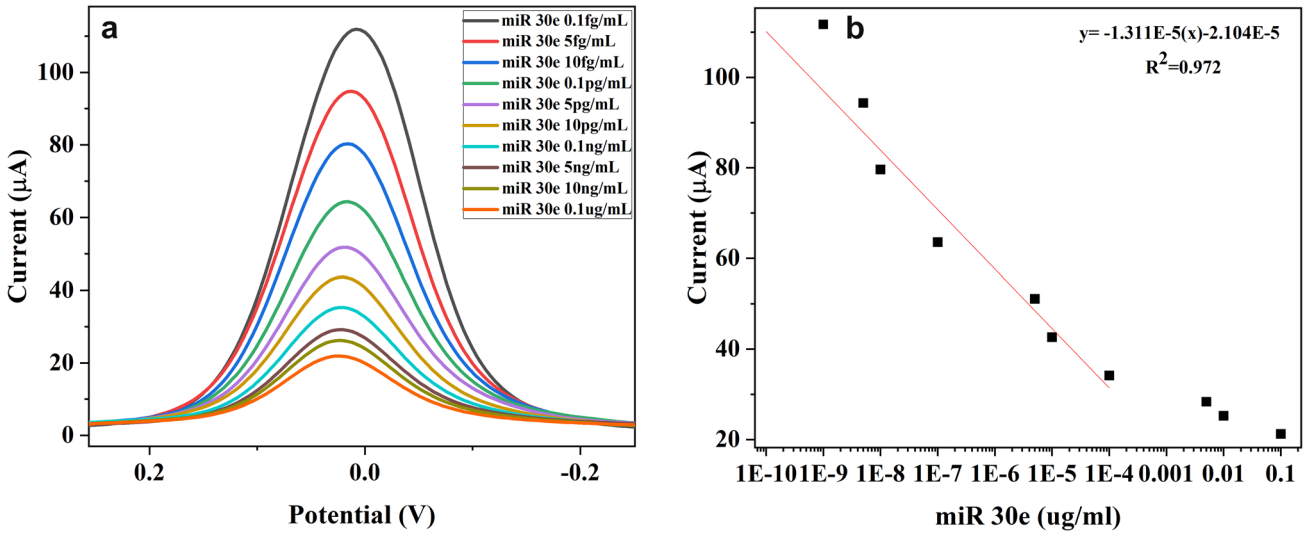

Fig. 5 **a** Differential pulse voltammetric response of fabricated biosensor at target miR30e concentrations in FBS sample ranging from 0.1 fg/mL to 0.1 μg/mL). **b** Corresponding calibration plot of peak current of pancreatic biomarkers miR196a [35] and miR106a [49] displayed linear range of 50 aM–50 pM and 1 fM–1 nM and LOD of 15 aM and 0.3 fM, respectively. Present DPV analysis exhibits comparable linear range from (149 aM to 14.9 nM) and LOD as 14.9 aM

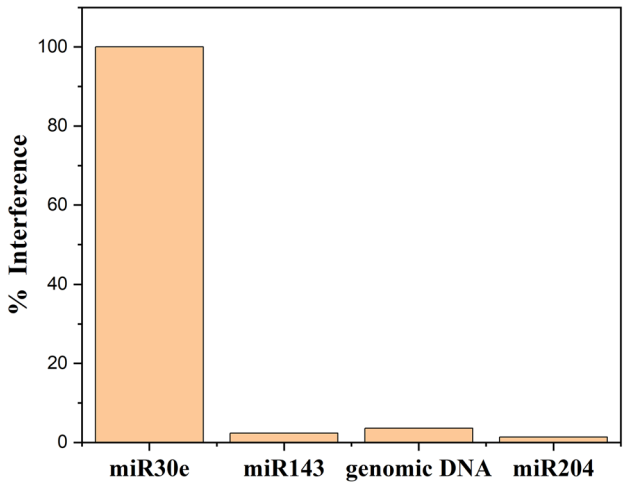

Fig. 6 Percentage interference from non-complementary sequences (miR 143, miR 204) and scrambled genomic DNA sequence (negative control) in comparison to complementary (miR30e)

DPV-based immunosensor exhibit wide linear range and dynamic range hence suitable for diagnostic purpose of screening, early detection and timely treatment of cancer. In addition to this, the developed biosensor can serve the purpose of a cost-effective, convenient, and non-invasive tool. However, none of the miRNA is specific since they are upregulated or downregulated in other conditions as well. Future work can be directed towards development of biosensor using panel of miRNAs or a mixed panel of miRNA, protein and ctDNA to achieve specificity and sensitivity of cancer diagnosis.

Acknowledgements Namita is thankful to Jaypee Institute of Information Technology Noida, India for providing research fellowship and other research facilities for completion of this project. The authors are also thankful to advanced instrumentation and research facility (AIRF), Jawaharlal Nehru University for extending the facility for transmission electron microscopy analysis.

Declarations

Conflict of Interest The authors declare no conflict of interest.

References

1. Gaidhani RH, Balasubramaniam G (2021) An epidemiological review of pancreatic cancer with special reference to India. Indian J Med Sci 73(1):99–109. https://doi.org/10.25259/IJMS_92_2020
2. Rickes S, Unkrodt K, Neye H, Ocran KW, Wermke W (2002) Differentiation of pancreatic tumours by conventional ultrasound, unenhanced and echo-enhanced power Doppler sonography. Scand J Gastroenterol 37(11):1313–1320. https://doi.org/10.1080/003655202761020605
3. Palazzo L, Roseau G, Gayet B, Vilgrain V, Belghiti J, Fékéte F, Paolaggi JA (1993) Endoscopic ultrasonography in the diagnosis and staging of pancreatic adenocarcinoma. Results of a prospective study with comparison to ultrasonography and CT scan. Endoscopy 25(2):143–150. https://doi.org/10.1055/s-2007-1010273
4. Sendler A, Avril N, Helmberger H, Stollfuss J, Weber W, Bengel F, Schwaiger M, Roder JD, Siewert JR (2000) Preoperative evaluation of pancreatic masses with positron emission tomography using 18F-fluorodeoxyglucose: diagnostic limitations. World J Surg 24(9):1121–1129. https://doi.org/10.1007/s002680010182
5. Hamada S, Shimosegawa T (2011) Biomarkers of pancreatic cancer. Pancreatology 11(suppl 2):14–19. https://doi.org/10.1159/000323479

6. Simeone DM, Ji B, Banerjee M, Arumugam T, Li D, Anderson MA, Bamberger AM, Greenson J, Brand RE, Ramachandran V, Logsdon CD (2007) CEACAM1, a novel serum biomarker for pancreatic cancer. Pancreas 34(4):436–443. https://doi.org/10.1097/mpa.0b013e3180333ae3
7. Kunovsky L, Tesarikova P, Kala Z, Kroupa R, Kysela P, Dolina J, Trna J (2018) The use of biomarkers in early diagnostics of pancreatic cancer. Can J Gastroenterol Hepatol. https://doi.org/10.1155/2018/5389820
8. Tempero MA, Malafa MP, Al-Hawary M et al (2017) Pancreatic adenocarcinoma, version 2.2017, NCCN clinical practice guidelines in oncology. J Natl Compr Canc Netw 15(8):1028–1061. https://doi.org/10.6004/jnccn.2017.0131
9. Bunduc S, Gede N, Váncsa S, Lillik V, Kiss S, Dembrovszky F, Eróss B, Szakács Z, Gheorghe C, Mikó A, Hegyi P (2022) Prognostic role of cell-free DNA biomarkers in pancreatic adenocarcinoma: a systematic review and meta–analysis. Crit Rev Oncol Hematol 169:103548. https://doi.org/10.1016/j.critrevonc.2021.103548
10. Brancaccio M, Natale F, Falco G, Angrisano T (2019) Cell-free DNA methylation: the new frontiers of pancreatic cancer biomarkers'. Discov Genes 11(1):14. https://doi.org/10.3390/genes11010014
11. Lee RC, Feinbaum RL, Ambros V (1993) The *C. elegans* heterochronic gene lin-4 encodes small RNAs with antisense complementarity to lin-14. Cell 75(5):843–854. https://doi.org/10.1016/0092-8674(93)90529-y
12. Reinhart BJ, Slack FJ, Basson M, Pasquinelli AE, Bettinger JC, Rougvie AE, Horvitz HR, Ruvkun G (2000) The 21-nucleotide let-7 RNA regulates developmental timing in *Caenorhabditis elegans*. Nature 403(6772):901–906. https://doi.org/10.1038/35002607
13. Pasquinelli AE, Reinhart BJ, Slack F, Martindale MQ, Kuroda MI, Maller B, Hayward DC, Ball EE, Degnan B, Müller P, Spring J, Srinivasan A, Fishman M, Finnerty J, Corbo J, Levine M, Leahy P, Davidson E, Ruvkun G (2000) Conservation of the sequence and temporal expression of let-7 heterochronic regulatory RNA. Nature 408(6808):86–89. https://doi.org/10.1038/35040556
14. Lagos-Quintana M, Rauhut R, Lendeckel W, Tuschl T (2001) Identification of novel genes coding for small expressed RNAs. Science 294(5543):853–858. https://doi.org/10.1126/science.1064921
15. Trang P, Weidhaas JB, Slack FJ (2008) MicroRNAs as potential cancer therapeutics. Oncogene 27(Suppl 2):S52-57. https://doi.org/10.1038/onc.2009.353
16. Slater PE, Strauch K, Rospleszcz S, Ramaswamy A, Esposito I, Klöppel G, Matthäi E, Heeger K, Fendrich V, Langer P, Bartsch DK (2014) MicroRNA-196a and -196b as potential biomarkers for the early detection of familial pancreatic cancer. Translational Oncology 7(4):464–471. https://doi.org/10.1016/j.tranon.2014.05.007
17. Ishige F, Hoshino I, Iwatate Y et al (2020) MIR1246 in body fluids as a biomarker for pancreatic cancer. Sci Rep 10(1):1–7. https://doi.org/10.1038/s41598-020-65695-6
18. Yu Y, Tong Y, Zhong A, Wang Y, Lu R, Guo L (2020) Identification of Serum microRNA-25 as a novel biomarker for pancreatic cancer. Medicine 99(52):e23863. https://doi.org/10.1097/MD.0000000000023863
19. Zhang J, Zhao CY, Zhang SH, Yu DH, Chen Y, Liu QH, Shi M, Ni CR, Zhu MH (2014) Upregulation of miR194 contributes to tumor growth and progression in pancreatic ductal adenocarcinoma. Oncol Rep 31(3):1157–1164. https://doi.org/10.3892/or.2013.2960
20. Zhao C, Zhang J, Zhang S, Yu D, Chen Y, Liu Q, Shi M, Ni C, Zhu M (2013) Diagnostic and biological significance of microRNA-192 in pancreatic ductal adenocarcinoma. Oncol Rep 30(1):276–284. https://doi.org/10.3892/or.2013.2420
21. Panarelli NC, Chen YT, Zhou XK, Kitabayashi N, Yantiss RK (2012) MicroRNA expression aids the preoperative diagnosis of pancreatic ductal adenocarcinoma. Pancreas 41(5):685–690. https://doi.org/10.1097/MPA.0b013e318243a905
22. Li F, Xu JW, Wang L, Liu H, Yan Y, Hu SY (2017) MicroRNA-221-3p is up-regulated and serves as a potential biomarker in pancreatic cancer. Artif Cells Nanomed Biotechnol 46(3):482–487. https://doi.org/10.1080/21691401.2017.1315429
23. Morimura R, Komatsu S, Ichikawa D, Takeshita H, Tsujiura M, Nagata H, Konishi H, Shiozaki A, Ikoma H, Okamoto K, Ochiai T, Taniguchi H, Otsuji E (2011) Novel diagnostic value of circulating miR18a in plasma of patients with pancreatic cancer. Br J Cancer 105(11):1733–1740. https://doi.org/10.1038/bjc.2011.453
24. Li A, Yu J, Kim H, Wolfgang CL, Canto MI, Hruban RH, Goggins M (2013) MicroRNA array analysis finds elevated serum miR 1290 accurately distinguishes patients with low-stage pancreatic cancer from healthy and disease controls. Clin Cancer Res 19(13):3600–3610. https://doi.org/10.1158/1078-0432.CCR-12-3092
25. Hussein NA, Kholy ZA, Anwar MM, Ahmad MA, Ahmad, (2017) Plasma miR-22-3p, miR-642b-3p and miR-885-5p as diagnostic biomarkers for pancreatic cancer. J Cancer Res Clin Oncol 143(1):83–93. https://doi.org/10.1007/s00432-016-2248-7
26. Li A, Omura N, Hong SM, Vincent A, Walter K, Griffith M, Borges M, Goggins M (2010) Pancreatic cancers epigenetically silence SIP1 and hypomethylate and overexpress miR200a/200b in association with elevated circulating miR200a and miR200b levels. Cancer Res 70(13):5226–5237. https://doi.org/10.1158/0008-5472.CAN-09-4227
27. Khan IA, Rashid S, Singh N, Rashid S, Singh V, Gunjan D, Das P, Dash NR, Pandey RM, Chauhan SS, Gupta S, Saraya A (2021) Panel of serum miRNAs as potential non-invasive biomarkers for pancreatic ductal adenocarcinoma. Sci Rep 11(1):1–10. https://doi.org/10.1038/s41598-021-82266-5
28. Cote GA, Gore AJ, McElyea SD, Heathers LE, Xu H, Sherman S, Korc M (2014) A pilot study to develop a diagnostic test for pancreatic ductal adenocarcinoma based on differential expression of select miRNA in plasma and bile. Am J Gastroenterol 109(12):1942–1952. https://doi.org/10.1038/ajg.2014.331
29. Shao H, Zhang Y, Yan J, Ban X, Fan X, Chang X, Lu Z, Wu Y, Zong L, Mo S, Yu S, Chen J (2021) Upregulated microRNA-483-3p is an early event in pancreatic ductal adenocarcinoma (PDAC) and as a powerful liquid biopsy biomarker in PDAC. Onco Targets Ther 14:2163–2175. https://doi.org/10.2147/OTT.S288936
30. Xu J, Cao Z, Liu W, You L, Zhou L, Wang C, Lou W, Sun B, Miao Y, Liu X, Zhang T, Zhao Y (2016) Plasma miRNAs effectively distinguish patients with pancreatic cancer from controls. Ann Surg 263(6):1173–1179. https://doi.org/10.1097/SLA.0000000000001345
31. Debernardi S, Massat NJ, Radon TP, Sangaralingam A, Banissi A, Ennis DP, Dowe T, Chelala C, Pereira SP, Kocher HM, Young BD, Bond-Smith G, Hutchins R, Crnogorac-Jurcevic T (2015) Noninvasive urinary miRNA biomarkers for early detection of pancreatic adenocarcinoma. Am J Cancer Res 5(11):3455–3466 (**PMID: 26807325**)
32. Xia N, Zhang L (2014) Nanomaterials-based sensing strategies for electrochemical detection of microRNAs. Materials (Basel) 7(7):5366–5384. https://doi.org/10.3390/ma7075366
33. Yammouri G, Mohammadi H, Amine A (2019) A highly sensitive electrochemical biosensor based on carbon black and gold nanoparticles modified pencil graphite electrode for microRNA-21 detection. Chem Afr 2:291–300. https://doi.org/10.1007/s42250-019-00058-x

34. Chen SC, Chen KT, Fang-Ju Jou A (2021) Polydopamine-gold composite based electrochemical biosensor using dual-amplification strategy for detecting pancreatic cancer-associated microRNA. Biosens Bioelectron 173:112815. https://doi.org/10.1016/j.bios.2020.112815
35. Guo J, Yuan C, Yan Q, Duan Q, Li X, Yi G (2018) An electrochemical biosensor for microRNA-196a detection based on cyclic enzymatic signal amplification and template-free DNA extension reaction with the adsorption of methylene blue. Biosens Bioelectron 105:103–108. https://doi.org/10.1016/j.bios.2018.01.036
36. Zeng D, Wang Z, Meng Z, Wang P, San L, Wang W, Aldalbahi A, Li L, Shen J, Mi X (2017) DNA tetrahedral nanostructure-based electrochemical miRNA biosensor for simultaneous detection of multiple miRNAs in pancreatic carcinoma. ACS Appl Mater Interfaces 9(28):24118–24125. https://doi.org/10.1021/acsami.7b05981
37. Mao L, Liu S, Hu L (2018) miR30 family: a promising regulator in development and disease. Biomed Res Int. https://doi.org/10.1155/2018/9623412
38. Liu Mm, Li Z, Han Xd et al (2017) MiR30e inhibits tumor growth and chemoresistance via targeting IRS1 in Breast Cancer. Sci Rep 7(1):1–10. https://doi.org/10.1038/s41598-017-16175-x
39. Wang Z, Zhang J, Zhang S, Yan S, Wang Z, Wang C, Zhang X (2019) MiR30e and miR92a are related to atherosclerosis by targeting ABCA1. Mol Med Rep 19(4):3298–3304. https://doi.org/10.3892/mmr.2019.9983
40. Hu W, Yao W, Li H, Chen L (2020) MiR30e-5p inhibits the migration and invasion of nasopharyngeal carcinoma via regulating the expression of MTA1. Biosci Rep. https://doi.org/10.1042/BSR20194309
41. Bhattacharya S, Steele R, Shrivastava S (2015) Serum miR30e and miR223 as novel noninvasive biomarkers for hepatocellular carcinoma. Am J Pathol 186(2):242–247. https://doi.org/10.1016/j.ajpath.2015.10.003
42. Dieter C, Assmann TS, Costa AR, Canani LH, de Souza BM, Bauer AC, Crispim D (2019) MiR30e-5p and MiR15a-5p expressions in plasma and urine of type 1 diabetic patients with diabetic kidney disease. Front Genet. https://doi.org/10.3389/fgene.2019.00563
43. Leva-Bueno J, Peyman SA, Millner PA (2020) A review on impedimetric immunosensors for pathogen and biomarker detection. Med Microbiol Immunol 209(3):343–362. https://doi.org/10.1007/s00430-020-00668-0
44. Ramos MDM, Correia MGH (2011) Electric field induced charge transfer through single- and double-stranded DNA polymer molecules. Soft Matter 7:10091–10099. https://doi.org/10.1039/C1SM05641G
45. Asadzadeh-Firouzabadi A, Zare HR (2017) Application of cysteamine-capped gold nanoparticles for early detection of lung cancer-specific miRNA (miR25) in human blood plasma. Anal Methods 9(25):3852–3861. https://doi.org/10.1039/C7AY01098B
46. Zhuravel R, Huang H, Polycarpou G, Polydorides S, Motamarri P, Katrivas L, Rotem D, Sperling J, Zotti LA, Kotlyar AB, Cuevas JC, Gavini V, Skourtis SS, Porath D (2020) Backbone charge transport in double-stranded DNA. Nat Nanotechnol 15:836–840. https://doi.org/10.1038/s41565-020-0741-2
47. Chandra S, Adeloju S (2020) A new sensor for detecting microrna 133b (Parkinson's disease biomarker). Sens Int 1:100005. https://doi.org/10.1016/j.sintl.2020.100005
48. Zouari M, Campuzano S, PingarronN RN (2018) Amperometric biosensing of miRNA21 in serum and cancer cells at nanostructured platforms using Anti-DNA−RNA hybrid antibodies. ACS Omega 3:8923–8931. https://doi.org/10.1021/acsomega.8b00986
49. Daneshpour M, Omidfar K, Ghanbarian H (2016) A novel electrochemical nanobiosensor for the ultrasensitive and specific detection of femtomolar-level gastric cancer biomarker miRNA106a. Beilstein J Nanotechnol 7:2023–2036. https://doi.org/10.3762/bjnano.7.193

Authors and Affiliations

Namita Sharma[1] · Sudha Srivastava[1]

✉ Sudha Srivastava
sudha.srivastava@jiit.ac.in

Namita Sharma
nsharma2728@gmail.com

[1] Department of Biotechnology, Jaypee Institute of Information Technology, A-10, Sector-62, Noida, UP, India